Energy Engineering

Tech Science Press

Doi:10.32604/ee.2025.072773

ARTICLE

A Coordinated Thermal Power-Energy Storage Planning Method for Addressing Renewable Energy Uncertainty

Cheng Yang[1], Xiuyu Yang[1,*], Gangui Yan[1], Hongda Dong[2] and Chenggang Li[2]

[1]School of Electrical Engineering, Northeast Electric Power University, Jilin, 132012, China
[2]Electric Power Research Institute, State Grid Jilin Electric Power Company Limited, Changchun, 130021, China
*Corresponding Author: Xiuyu Yang. Email: yangxiuyu2011@163.com

Received: 03 September 2025; Accepted: 13 November 2025; Published: 27 April 2026

ABSTRACT: The integration of renewable energy introduces significant uncertainty into daily power system operation scenarios. Traditional deterministic unit commitment methods struggle to adapt to these conditions, often resulting in poor economic performance and high curtailment rates in planning outcomes. To address these challenges, this paper proposes a coordinated thermal power-energy storage planning methodology for managing renewable energy uncertainty. First, the operational effectiveness of daily unit commitment under uncertain renewable energy scenarios is analyzed, with quantitative assessment of how different commitment strategies impact supply-demand balance and economic performance. Subsequently, by conducting flexibility evaluation under multiple renewable energy output profiles in typical days, an entropy weight-based method for determining daily unit commitment is developed. This approach evaluates the performance of commitment strategies across multiple uncertain scenarios using various flexibility metrics, enabling the identification of strategies that effectively accommodate uncertainty. Furthermore, building upon the entropy weight-based unit commitment methodology, a coordinated thermal power-energy storage planning model is formulated with the objective of minimizing expected costs across all scenarios. Finally, using actual measurement data from a Northeast China power grid, multiple typical-day uncertainty scenarios are constructed, and case study analysis validates the effectiveness of the proposed methodology.

KEYWORDS: RE uncertainty; joint fire-storage planning; entropy weighting method; flexibility evaluation

1 Introduction

The output of renewable energy is highly volatile and uncertain due to its dependence on meteorological and geographical conditions. The large-scale integration of renewable energy intensifies system uncertainty [1,2], making real-time power balance increasingly difficult and leading to frequent extreme events of supply–demand imbalance [3], Consequently, high-penetration renewable energy power systems are facing the dual challenges of ensuring supply security and renewable energy utilization.

The deployment of flexible resources such as energy storage is an effective measure to enhance system flexibility and mitigate the impact of renewable energy uncertainty. During planning, underestimating the degree of renewable output uncertainty may reduce investment costs in flexibility resources but could result in insufficient regulation capability, frequent power shortages, and large-scale curtailment events. Conversely, overestimating uncertainty could lead to excessive investment in flexibility resources, resulting in redundancy and economic inefficiency. Therefore, configuration schemes based on a single deterministic renewable output scenario are insufficient to address the wide range of possible fluctuations. Properly

considering multiple uncertainty scenarios of renewable generation is essential for ensuring the secure and economic operation of future high-renewable energy power systems.

Extensive research has been conducted on power generation and energy storage planning under renewable energy uncertainty, mainly categorized into stochastic programming, robust optimization, and multi-scenario analysis methods. Stochastic programming represents renewable energy variability through probabilistic distributions. For example, reference [4] models net-load uncertainty using probability distributions and incorporates it into optimization through the concept of admissible regions. Reference [5] introduces probabilistic intervals to represent wind power uncertainty and evaluates risks using Conditional Value-at-Risk (CVaR). Reference [6] considers uncertainties in generation, load, and market factors under a power market environment and solves probabilistic constraints via a Monte Carlo simulation-based heuristic algorithm. However, the accuracy of stochastic programming largely depends on the correctness of the assumed probability distribution. Given the complex and non-stationary characteristics of wind and solar output [7,8], it is difficult to model their distributions precisely. Moreover, extracting distribution functions from historical data or Monte Carlo-generated scenarios may distort the temporal correlations inherent in renewable energy output, thus diminishing the effectiveness of the resulting planning schemes in addressing uncertainty.

Robust optimization approaches model renewable energy uncertainty as uncertainty sets and seek optimal solutions under worst-case conditions. Reference [9] develops a three-level robust planning model that employs energy storage to mitigate the impact of wind power investment uncertainty and the retirement of thermal units on system reserves. Reference [10] introduces a leader–follower game approach with ellipsoidal uncertainty sets to model offshore wind generation uncertainty. Reference [11] constrains forecast deviations within bounds determined by system uncertainty levels, while reference [12] incorporates energy storage lifetime constraints to prevent overly optimistic planning results, though uncertainty is only considered on the load side. Robust optimization effectively enhances system security [13]; however, its focus on worst-case scenarios often leads to overly conservative and economically suboptimal solutions.

Multi-scenario analysis methods have also been widely applied in uncertainty-based power system planning [14–16]. Reference [17] employs a high-resolution assessment model to capture the multidimensional impacts of renewable output uncertainty on system operation. Reference [18] uses machine learning to generate renewable output scenarios with temporal characteristics, developing a coordinated planning model for wind–solar–storage systems that preserves long-term correlations. Reference [19] applies the K-Medoids clustering method to reduce scenario numbers and guide energy storage configuration for wind and solar smoothing. However, most existing studies focus on "one-to-one" relationships between load and renewable generation, which become inadequate as renewable penetration increases and system uncertainty diversifies.

As an objective weighting approach, the entropy weight method has been widely applied across various fields [20,21]. At the same time, compared with the analytic hierarchy process (AHP), the entropy weight method is completely based on the degree of data variation to determine the index weight, which avoids the deviation caused by subjective judgment in AHP and makes the weight distribution more objective. When dealing with multi-index decision-making related to renewable energy uncertainty, the objectivity of data is very important, and the entropy weight method can better reflect the actual importance of each index. Compared with the fuzzy comprehensive evaluation method, the entropy weight method is more concise and clear in the face of complex index system, and does not need to construct complex fuzzy relation matrix and fuzzy synthesis operation, which has significant advantages in dealing with large-scale data and multi-index power system planning problems. Through these comparative analyses, the rationality and applicability of choosing entropy weight method to manage the uncertainty of renewable energy and apply it to the joint planning model of fire and energy storage are highlighted.

In summary, to address the challenge of efficient thermal–storage co-optimization under high renewable penetration and strong uncertainty, this paper proposes a thermal–storage coordinated planning method based on the entropy weight theory. First, the adaptability of conventional unit commitment plans under different renewable scenarios is analyzed. A set of flexibility evaluation indices is established to assess the adaptability of various unit commitment schemes, and the entropy weight method is employed to assign objective weights to these indices, thus identifying the most comprehensive and robust unit commitment plan. Second, based on a "one-to-many" principle, multiple renewable generation scenarios are associated with each typical load curve. The optimal storage configuration is then determined by minimizing the expected total cost over the entire planning horizon. Finally, a case study based on a regional power grid in Northeast China is conducted to validate the effectiveness and superiority of the proposed method.

2 Determining Thermal Power Unit Commitment Based on Entropy Weight

2.1 Rational Selection of Daily Unit Commitment

The power output of a thermal power unit must be maintained within its maximum and minimum technical limits. Consequently, its regulation capability is constrained by the daily unit commitment schedule. Under a given scenario, this section illustrates the relationship between the daily commitment of thermal power units and the resulting power curtailment and power shortage, without considering the impact of unit ramping rates for now.

As shown in Fig. 1, two different unit commitment schedules under the same net load curve are illustrated. In Fig. 1a, the maximum value of the net load is set as the daily unit commitment. The blue area represents the adjustable range of the thermal power units. The portion of the net load curve below the blue area indicates power curtailment, while power shortage does not occur in this case. In Fig. 1b, the committed capacity of the thermal power units is reduced, with the minimum output set as close as possible to the daily minimum net load. The adjustable range of the thermal power units then becomes the red area. The portion of the net load curve above the red area corresponds to power shortage, and power curtailment is absent under this configuration.

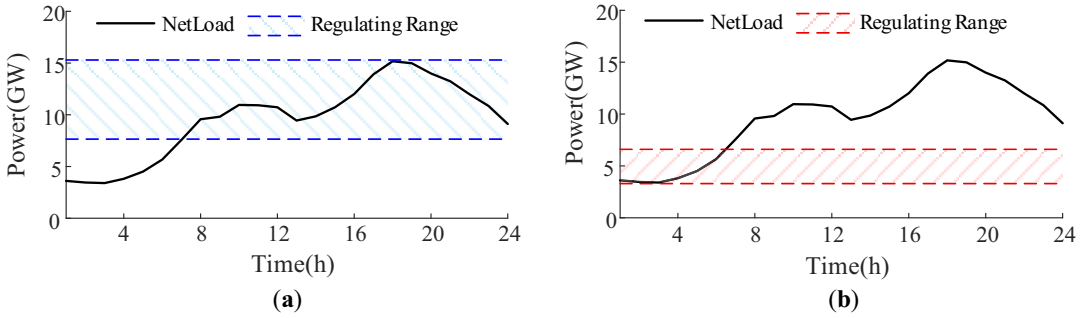

Figure 1: The effect of different start-up plans in a certain scenario: (**a**) Maximum net load plan; (**b**) Minimum net load plan

Based on these two daily unit commitment schedules, the role of energy storage systems is analyzed, under the assumption that the system is equipped with adequate energy storage capacity.

Fig. 2 illustrates the system's power curtailment and power shortage scenarios with the participation of energy storage. The green dashed line in the figure represents the net load curve after the action of the energy storage system. In Fig. 2a, the energy storage charges during periods of power curtailment and discharges during peak net load periods, thereby resolving the power curtailment issue. However, in this case, the

regulation range of the thermal power units significantly exceeds the maximum value of the adjusted net load. If the committed capacity were reduced, both the system's power curtailment and the demand for energy storage would be further decreased. Fig. 2b presents a scenario under a different daily unit commitment schedule. Here, the committed capacity of the thermal power units is too low, leaving no charging headroom for the energy storage system and thus failing to alleviate the power shortage. In practice, an appropriate daily unit commitment schedule for thermal power units should exist, which would enable the thermal power–energy storage system to avoid both power curtailment and power shortage, without overstating the system's requirement for energy storage capacity.

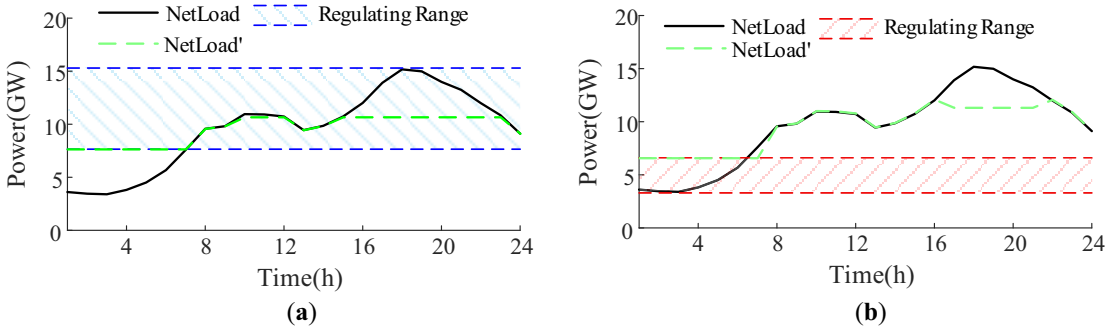

Figure 2: Impact of different unit commitment schemes on the action space of energy storage: (**a**) Maximum net load scheme; (**b**) Minimum net load scheme

As shown in Fig. 3, a slight reduction in the committed capacity of thermal power units leads to the coexistence of both power curtailment and power shortage. However, sufficient charging and discharging headroom is available for the energy storage system. With the participation of energy storage in regulation, both power curtailment and power shortage can be fully mitigated without requiring excessive energy storage resources. By properly determining the daily unit commitment schedule for thermal power units to achieve effective coordination between thermal generation and energy storage, the system's regulation capability can be fully utilized. This approach ensures adequate system flexibility while optimizing investment costs.

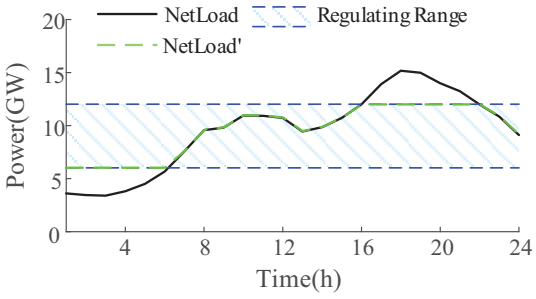

Figure 3: Schematic diagram of coordinated operation between thermal power units and energy storage

2.2 Impact of Renewable Energy Uncertainty on Daily Unit Commitment

In conventional power systems with low renewable energy penetration, the generation side is nearly fully dispatchable, and the primary source of system uncertainty lies in load variability. In contrast, in future power systems with a high share of renewable energy, the uncertainty of renewable generation will become the dominant factor affecting system operation. Currently, in power system operation and planning, load forecasting has achieved a high level of accuracy. Therefore, the major challenge in operating

a high-renewable power system will be addressing the significant uncertainty associated with renewable energy sources.

Fig. 4 illustrates three renewable energy scenarios considered in the scheduling day. Scenario 3 represents a conventional case with a high probability of occurrence, while Scenarios 1 and 2 correspond to scenarios with extremely high and extremely low renewable energy generation, respectively. Each scenario presents distinct operational challenges. In Scenario 1, characterized by high renewable generation, the output profile closely aligns with the system load curve. Although generation resources are sufficient in this case, there is a risk of renewable energy curtailment. In Scenario 3, where renewable output is very low and even approaches zero during certain periods, the system experiences significant supply pressure, leading to a risk of power shortage. Developing an appropriate unit commitment strategy to comprehensively address the varying flexibility requirements across these multiple scenarios will significantly influence both the security and economic efficiency of system operation.

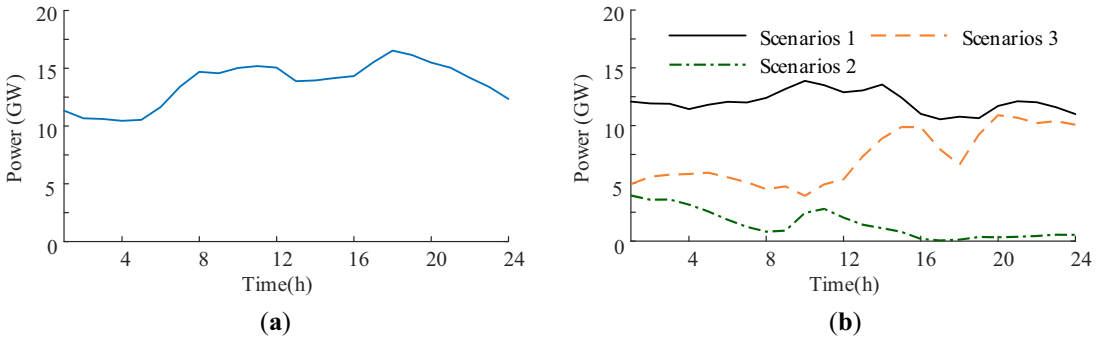

Figure 4: Schematic diagram of a daily dispatchable load profile and renewable energy profile: (**a**) Load curve; (**b**) Renewable energy curve

Fig. 5 illustrates the net load curves under three scenarios and schematic representations of two unit commitment strategies. In Strategy 1, the maximum net load value across all possible scenarios is selected as the committed capacity. Strategy 2, in contrast, adopts the maximum net load value from Scenario 3, which has the highest probability of occurrence. Although Strategy 1 ensures power supply security during periods of extremely low renewable energy generation, it significantly exceeds the net load curve in conventional scenarios. Furthermore, the energy storage system lacks sufficient operational headroom, leading to substantial renewable energy curtailment. Strategy 2, however, fails to maintain power supply security in Scenario 1. In this scenario, the net load exceeds the maximum output of the thermal power units at 18 time intervals, resulting in a power shortage of 4633.73 kWh, which accounts for 14.11% of the total energy demand. Relying solely on energy storage is insufficient to ensure power supply security under these conditions. The unit commitment strategy derived from Scenario 1 is clearly impractical and is therefore excluded from further discussion.

2.3 Flexibility Evaluation Metrics

Power system flexibility must be evaluated from multiple dimensions, as it involves distinct requirements in terms of regulation direction, regulation capacity, and ramping rate. Fig. 6 provides a schematic diagram of these system flexibility requirements.

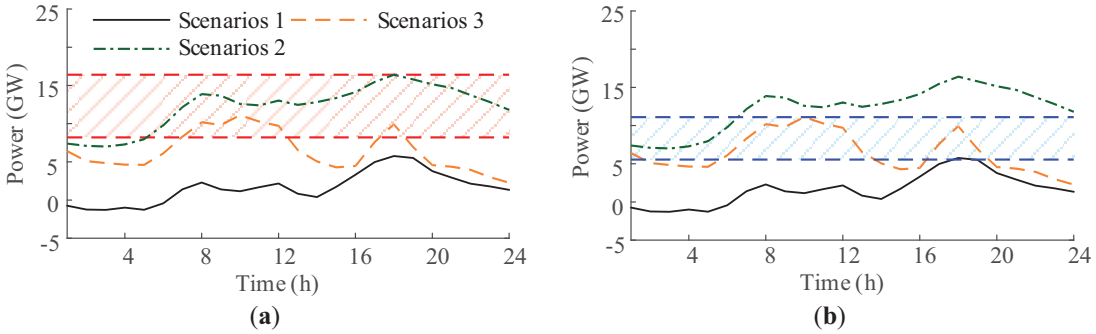

Figure 5: Comparison of the two unit commitment strategies: (**a**) Strategy A; (**b**) Strategy B

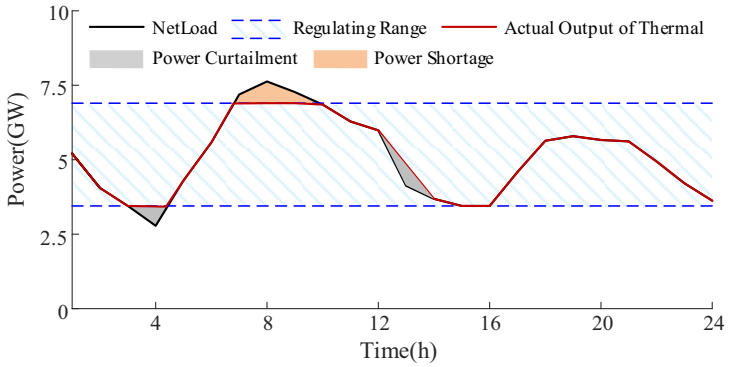

Figure 6: Schematic diagram of flexibility requirements

As shown in Fig. 6, the gray areas represent power curtailment while the yellow areas indicate power shortage, corresponding to the system's flexibility requirements in the downward and upward directions, respectively. Although both gray regions denote power curtailment, they originate from distinct causes, reflecting different aspects of system flexibility needs. The first gray area, where the net load falls below the adjustable range of the thermal power units, signifies a deficiency in regulation capacity. This issue can be addressed either by reducing the committed capacity of thermal power units or by deploying energy storage systems. The second gray area, occurring within the adjustable range of the thermal power units, results from insufficient downward ramping capability and highlights a need for enhanced regulation speed. Increasing the committed capacity to improve ramping rates would raise the lower regulation limit, making energy storage the only viable solution to mitigate this type of curtailment. Similarly, power shortage incidents may also arise from either insufficient regulation capacity or inadequate ramping rates. Therefore, to comprehensively evaluate the flexibility of different unit commitment strategies across various scenarios, this paper introduces eight flexibility evaluation metrics, considering two directions (upward and downward regulation), two dimensions (capacity and ramping rate), and two attributes (energy volume and duration). The specific metrics are as follows.

2.3.1 Expected Upward/Downward Flexibility Capacity Deficiency

$$\Delta P^{j}_{\mathrm{UFC},t} = \begin{cases} 0 & , P^{j}_{\mathrm{NET},t} \le U^{\max}_{i} \\ P^{j}_{\mathrm{NET},t} - U^{\max}_{i} & , P^{j}_{\mathrm{NET},t} > U^{\max}_{i} \end{cases} \tag{1}$$

$$E^i_{\mathrm{UFC}} = \sum_j \mathrm{Pr}_j \cdot \sum_{t=1}^{T} \Delta P^j_{\mathrm{UFC},t} \tag{2}$$

$$\Delta P^j_{\mathrm{DFC},t} = \begin{cases} U_i^{\min} - P^j_{\mathrm{NET},t} & , P^j_{\mathrm{NET},t} \le U_i^{\min} \\ 0 & , P^j_{\mathrm{NET},t} > U_i^{\min} \end{cases} \tag{3}$$

$$E^i_{\mathrm{DFC}} = \sum_j \mathrm{Pr}_j \cdot \sum_{t=1}^{T} \Delta P^j_{\mathrm{UDC},t} \tag{4}$$

where, E^i_{UFC}, E^i_{DFC} represent the expected upward and downward flexibility capacity deficiency of the system, respectively; $U_i^{\max}$, $U_i^{\min}$ denote the upper and lower output limits of the units under the i-th unit commitment strategy; and Pr_j indicates the probability of occurrence of the j-th scenario.

2.3.2 Expected Upward/Downward Flexibility Ramping Deficiency

$$\Delta P^j_{\mathrm{NET},t} = P^j_{\mathrm{NET},t} - P^j_{\mathrm{NET},t-1} \tag{5}$$

$$\Delta P^j_{\mathrm{UFR},t} = \begin{cases} 0, \Delta P^j_{\mathrm{NET},t} \le RU_i \\ \Delta P^j_{\mathrm{NET},t} - RU_i, \Delta P^j_{\mathrm{NET},t} > RU_i \end{cases} \tag{6}$$

$$E^i_{\mathrm{UFR}} = \sum_j \mathrm{Pr}_j \cdot \sum_{t=1}^{T} \Delta P^j_{\mathrm{UFR},t} \tag{7}$$

$$\Delta P^j_{\mathrm{DFR},t} = \begin{cases} RD_i - \Delta P^j_{\mathrm{NET},t} & , \Delta P^j_{\mathrm{NET},t} \le RD_i \\ 0 & , \Delta P^j_{\mathrm{NET},t} > RD_i \end{cases} \tag{8}$$

$$E^i_{\mathrm{DFR}} = \sum_j \mathrm{Pr}_j \cdot \sum_{t=1}^{T} \Delta P^j_{\mathrm{DFR},t} \tag{9}$$

where, $\Delta P^j_{\mathrm{NET},t}$ represents the net load variation of the system at time interval t; E^i_{UFR}, E^i_{DFR} denote the expected upward and downward flexibility ramping deficiency of the system, respectively; RU_i, RD_i indicate the maximum upward and downward ramping capabilities of the units under commitment strategy i.

2.3.3 Expected Duration of Upward/Downward Flexibility Capacity Deficiency

$$E^i_{\mathrm{UCH}} = \sum_j \mathrm{Pr}\left\{ P^j_{\mathrm{NET},t} > U_i^{\max} \right\} T \tag{10}$$

$$E^i_{\mathrm{DCH}} = \sum_j \mathrm{Pr}\left\{ P^j_{\mathrm{NET},t} < U_i^{\min} \right\} T \tag{11}$$

where, E^i_{UCH}, E^i_{DCH} represent the expected duration of upward and downward flexibility capacity deficiency in the system, respectively; $\mathrm{Pr}\{\ \}$ denotes the probability of scenario j satisfying the expression within the brackets; and T represents the scheduling horizon for a typical day, which is set to 24 h in this study.

2.3.4 Expected Duration of Upward/Downward Flexibility Ramping Deficiency

$$E^i_{\mathrm{URH}} = \sum_j \mathrm{Pr}\left\{ RU_i \le P^j_{\mathrm{NET},t} - P^j_{\mathrm{NET},t-1} \right\} T \tag{12}$$

$$E^i_{\mathrm{DRH}} = \sum_j \Pr\left\{P^j_{\mathrm{NET},t} - P^j_{\mathrm{NET},t-1} \le RD_i\right\} T \tag{13}$$

where, E^i_{URH}, E^i_{DRH} denote the expected duration of upward and downward flexibility ramping deficiency, respectively.

2.4 Evaluation and Formulation of Unit Commitment Based on Entropy Weight Method

As indicated by the preceding analysis, the selection of the daily unit commitment for thermal power units influences the operational space of energy storage systems. Moreover, when confronting uncertain scenarios, a commitment strategy designed for a single scenario is often inadequate to meet the flexibility requirements of other scenarios. Based on the eight flexibility evaluation metrics introduced in the previous section, the entropy weight method is employed to determine the weight of each metric, thereby enabling the selection of a daily unit commitment strategy capable of comprehensively addressing all scenarios. A key advantage of the entropy weight method lies in its ability to derive the weights of each metric in a rapid, robust, and entirely objective manner. Since the fundamental principle of this method is to measure the dispersion degree of data, it can effectively identify the evaluation metrics that exert the most significant influence on system flexibility—that is, the most critical regulation requirements of the system.

$$\mathbf{Y} = \begin{bmatrix} y_{11} & \cdots & y_{1j} \\ \vdots & \vdots & \vdots \\ y_{i1} & \cdots & y_{ij} \end{bmatrix} \tag{14}$$

where, Y represents the standardized matrix, and y_{ij} denotes the value of the standardized metric. After performing the standardization procedure, the proportion of data for each metric and the corresponding information entropy can be derived, as shown in Eqs. (15) and (16):

$$p_{ij} = \frac{y_{ij}}{\sum_i y_{ij}} \tag{15}$$

$$e_j = -\ln\left(\frac{1}{n}\right) \sum_{i=1}^{n} p_{ij} \ln p_{ij} \tag{16}$$

where, p_{ij} represents the proportion of the value corresponding to commitment strategy i in metric j; e_j denotes the information entropy contained in metric j, and n indicates the number of data points in each metric. The information entropy is then utilized to determine both the weight of each metric and the comprehensive score of each commitment strategy.

$$w_j = \frac{1 - e_j}{m - \sum e_j} \tag{17}$$

$$S_i = \sum w_j * y_{ij} \tag{18}$$

where, w_j represents the weight assigned to each metric, and S_i denotes the comprehensive score for each commitment strategy.

2.5 A Coordinated Planning Method for Thermal Power-Energy Storage Systems with Daily Unit Commitment Formulation

The core of determining the daily unit commitment lies in utilizing the flexibility metrics proposed in the previous section to quantify the flexibility imbalance under a given commitment strategy across multiple dimensions. The entropy weight method is then applied to assign corresponding weights to these metrics,

enabling a comprehensive evaluation of the strategy. Ultimately, the strategy with the highest comprehensive score—capable of adapting to multiple potential scenarios—is selected.

Upon determining the daily unit commitment for each typical day, the required new capacity of thermal power units can be established. Based on the finalized unit commitment schedules, energy storage system planning is subsequently performed. The detailed solution procedure is illustrated in Fig. 7.

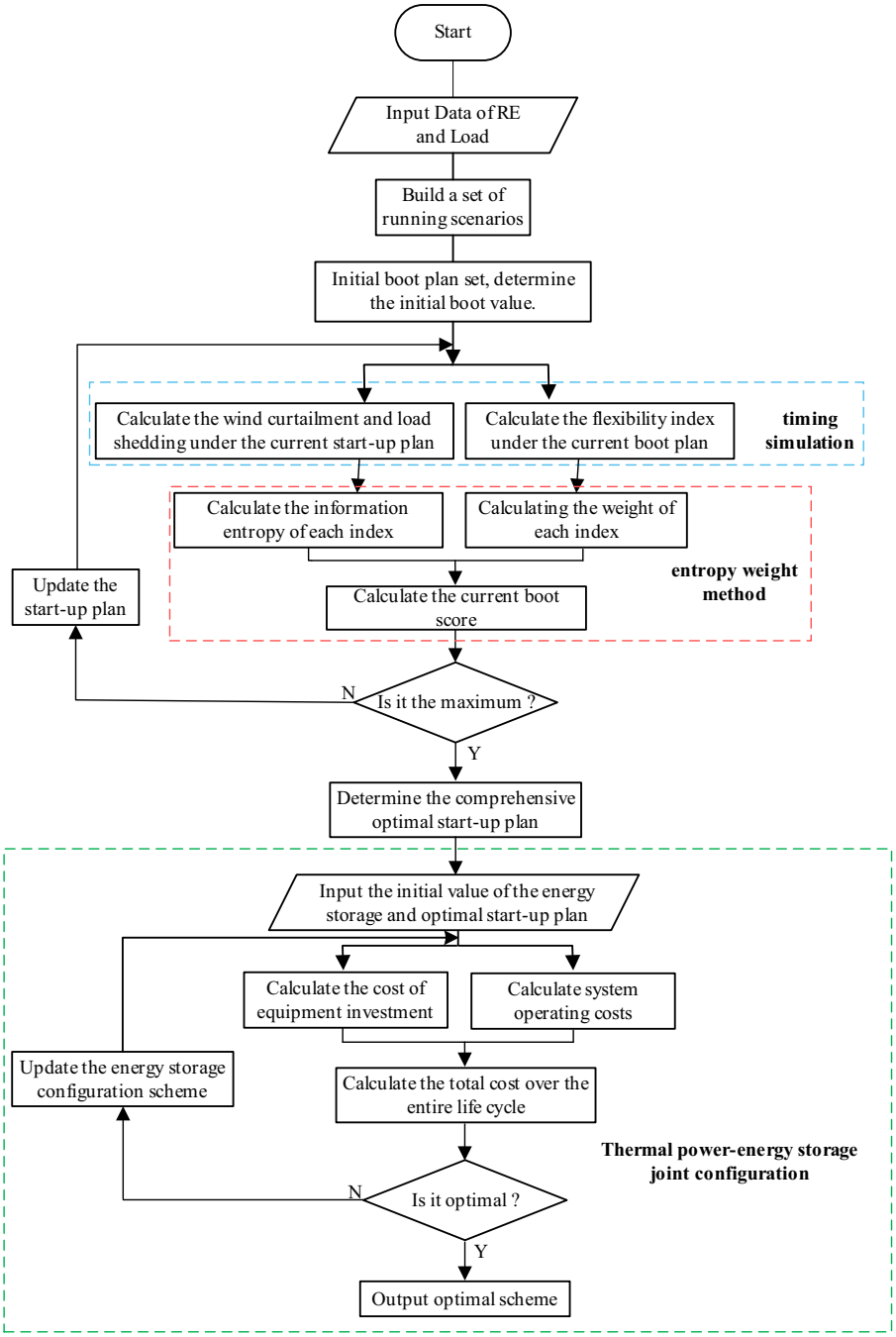

Figure 7: Flowchart of daily unit commitment and coordinated thermal power-energy storage planning

3 Thermal Power-Energy Storage Coordinated Planning Model

3.1 Objective Function

This paper adopts economic optimality as the planning objective. By comprehensively considering potential scenarios across all typical days, the economic performance of the planning outcome is evaluated based on the energy storage system construction cost and the expected operational cost throughout the planning horizon.

$$\min C = C_{\mathrm{OP}} + \left(C_{\mathrm{TH}} + C_{\mathrm{ESS}}\right) \cdot \frac{r\left(1+r\right)^{T_{\mathrm{plan}}}}{\left(1+r\right)^{T_{\mathrm{plan}}} - 1} \tag{19}$$

where, C_{TH} represents the construction cost of new thermal power units; C_{ESS} indicates the construction cost of energy storage device; C_{OP} represents the operating cost; r is discount rate.

$$C_{\mathrm{TH}} = c_{\mathrm{th}} P_{\mathrm{new}} \tag{20}$$

where, c_{th} denotes the unit capacity construction cost of thermal power units, and P_{new} represents the capacity of newly installed thermal power units.

The construction cost of the energy storage system comprises two components: the energy capacity cost and the power capacity cost, expressed as:

$$C_{\mathrm{ESS}} = c_{\mathrm{e}} E_{\mathrm{ess}} + c_{\mathrm{p}} P_{\mathrm{ess}} \tag{21}$$

where, c_{e}, c_{p} denote the unit energy capacity cost and unit power capacity cost of the energy storage system, respectively; E_{ess}, P_{ess} represent the energy capacity and power rating of the energy storage system in the planning solution.

The operational cost of the system should account for coal consumption costs, power curtailment costs, and power shortage costs across different scenarios. Considering the probability of each scenario, the expected operational cost is formulated as follows:

$$C_{\mathrm{OP}} = \mathbb{E}\left[c_{\mathrm{coal}} \sum P_g\right] + \mathbb{E}\left[c_{\mathrm{w}} \sum W_c\right] + \mathbb{E}\left[c_{\mathrm{L}} \sum L_c\right] \tag{22}$$

where, $\mathbb{E}[\cdot]$ denotes the mathematical expectation operator; c_{coal} represents the unit generation cost of thermal power units, and P_g indicates the corresponding power generation; c_{w} is the unit penalty for power curtailment, with W_c representing the curtailed power; c_{L} denotes the unit penalty for power shortage, and L_c signifies the power shortage level.

3.2 Operational Constraints

The model primarily considers the operational constraints of thermal power units, renewable energy units, energy storage systems, and system power balance. The detailed mathematical formulations are provided in Appendix B, while the economic and technical parameters for each unit type are summarized in Table A3.

4 Case Study

4.1 Fundamental Data and Typical Day Selection Methodology

Based on historical operational data from a power grid in Northeast China, where the current installed capacity of thermal power units is 16.5 GW, typical days have been extracted, with the projected renewable

energy penetration rate in the target year being approximately 41%. The original profiles of load, wind power, and photovoltaic output are presented in Fig. 8.

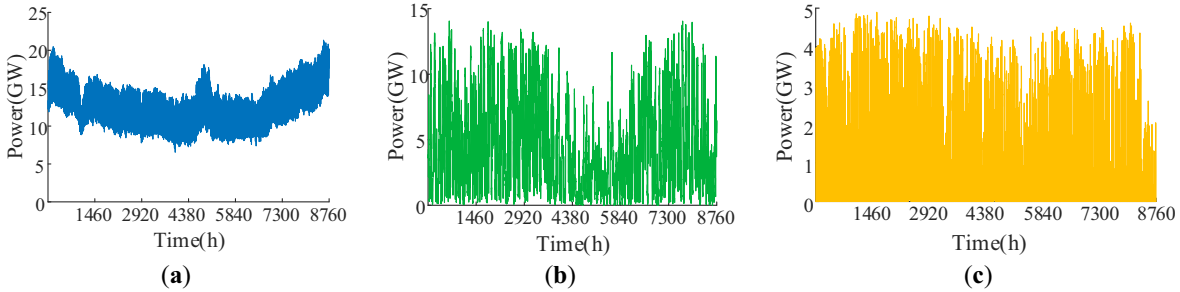

Figure 8: Original data profiles: (**a**) Load profile; (**b**) Wind power profile; (**c**) Photovoltaic power profile

Given the consistent fluctuation patterns of load curves across the system, which differ primarily in magnitude, this study identifies five distinct load profile types corresponding to five typical days. To account for the pronounced uncertainty of renewable energy, each typical day incorporates five renewable energy scenarios. A bi-level k-medoids clustering approach is employed to derive both the five typical days and the associated renewable energy generation scenarios for each day. The specific procedure is outlined as follows:

Step 1: Perform clustering on the annual load profiles from 365 days to obtain five cluster centers and their corresponding clusters, where each cluster member is indexed by its actual calendar date.

Step 2: Based on the resulting load clusters, categorize the annual wind and photovoltaic power profiles into five groups. Within each group, perform a second-level clustering to identify five cluster centers for wind and PV profiles, representing the potential renewable energy scenarios for each typical day.

The load and renewable energy generation profiles for each typical day are shown in the figure below, while the occurrence frequency of each typical day and the corresponding scenario probabilities are summarized in Table 1.

Table 1: Occurrence frequency of typical days and corresponding scenario probabilities

	RE 1	RE 2	RE 4	RE 5	Number of Days
Day 1	13.8%	19.5%	13.0%	9.8%	43.9%
Day 2	4.1%	10.8%	21.6%	27.0%	36.5%
Day 3	15.6%	44.4%	15.6%	8.9%	15.6%
Day 4	20.0%	25%	15.0%	10.0%	30.0%
Day 5	40.8%	20.4%	10.7%	19.4%	8.7%

The load and renewable energy output profiles for each typical day are presented in Appendix A Fig. A1. Based on this dataset and following different methodologies for determining the daily unit commitment of thermal power units, the following three planning cases are defined:

Case I: Considering renewable energy uncertainty, the entropy weight method is applied to determine the daily unit commitment for each typical day and the capacity of new thermal power units, followed by energy storage sizing.

Case II: Considering renewable energy uncertainty, both the capacity of new thermal power units and the energy storage system are determined by setting the daily unit commitment equal to the maximum possible net load value across all scenarios in each typical day.

Case III: Considering renewable energy uncertainty, the daily unit commitment is set as the maximum net load value from the most probable scenario within each typical day.

4.2 Planning Results for Case I

This case study incorporates the uncertainty of renewable energy and potential extreme scenarios encountered during actual system operation. The daily unit commitment for thermal power units is determined using the entropy weight method.

As illustrated in Fig. A1, considering the five net load scenarios within each typical day and assuming a unit capacity of 300 MW per thermal power unit, a set of candidate unit commitment strategies is constructed. This set ranges from the minimum number of units to the maximum number required to meet the peak net load (rounded up) across all scenarios for that typical day. Each candidate strategy is evaluated using the eight flexibility metrics proposed earlier. The entropy weight method dynamically determines the weight of each metric according to the specific conditions of each typical day. These weights are then used to calculate a comprehensive score for each candidate, enabling the selection of a final unit commitment strategy that is robust against varying load and renewable energy fluctuations.

As can be observed from Table 2, due to renewable energy fluctuations, significant variations exist in the maximum net load values across different typical days and even among various scenarios within the same typical day. Consequently, a unit commitment strategy based solely on the maximum net load of a single scenario proves inadequate for addressing the variability present in other scenarios. For instance, in Typical Day 2, the commitment strategy derived from Scenario 5 (the most probable scenario) fails to meet the power supply requirement in Scenario 2, while significantly exceeding the net load in Scenario 1, leading to substantial renewable energy curtailment.

Table 2: Maximum net load by scenario and typical day (GW)

	Scenario 1	Scenario 2	Scenario 3	Scenario 4	Scenario 5
Day 1	10.52	5.78	10.95	7.63	11.77
Day 2	4.31	15.17	12.19	9.77	14.45
Day 3	16.50	17.1	11.92	13.93	9.21
Day 4	15.02	19.46	15.58	10.85	18.82
Day 5	12.87	7.43	13.11	9.76	7.27

The entropy weight method is applied to determine the weight of each metric and to comprehensively evaluate the adaptability of each candidate strategy to multiple scenarios. The resulting metric weights and the corresponding optimal unit commitment strategy are presented in Tables 3 and 4, respectively.

Based on the optimal unit commitment strategy derived from Table 4, the capacity of new thermal power units is determined. Production simulation is then performed to obtain the required energy storage capacity and power rating, along with corresponding operational simulation results.

As shown in Table 5, the total annualized construction cost for the thermal power and energy storage systems amounts to 3.42 billion CNY/year, while the annual operating cost totals 23.39 billion CNY/year.

Table 3: Metric weights for Case I

	Day 1	Day 2	Day 3	Day 4	Day 5
E_{DCH}	0.031	0.046	0.049	0.039	0.034
E_{DFC}	0.053	0.064	0.076	0.056	0.069
E_{UCH}	0.103	0.098	0.083	0.065	0.164
E_{UFC}	0.192	0.175	0.151	0.122	0.280
E_{URH}	0.169	0.109	0.200	0.154	0.099
E_{UFR}	0.264	0.160	0.227	0.165	0.166
E_{DRH}	0.078	0.155	0.093	0.188	0.075
E_{DFR}	0.109	0.193	0.120	0.211	0.113

Table 4: Daily unit commitment for Case I

Day	1	2	3	4	5
Daily unit commitment (GW)	10.5	15	13.2	17.4	12

Table 5: Case I planning results

	Capacity	Cost/billion CNY
New thermal power units	0.9 GW	0.58
ESS	3.38 GW/13.5 GWh	2.84
E_{Pg}	73,473.56 GWh	16.9
E_{Wc}	7329.93 GWh	6.08
E_{Lc}	40.50 GWh	0.41
Total cost		26.81

4.3 Case II Planning Results

In this case study, the entropy weight method is not employed. Instead, the maximum net load value from all forecast scenarios in each typical day is directly adopted as the unit commitment strategy for energy storage sizing. The resulting daily unit commitment schedules for all typical days are provided in Table 6.

Table 6: Daily unit commitment for Case II

Day	1	2	3	4	5
Daily unit commitment (GW)	12	15.3	17.4	19.5	13.2

As presented in Table 7, the maximum net load commitment strategy is implemented, requiring 3 GW of new thermal power capacity. However, due to the severe compression of the operational space for energy storage, the configured energy storage capacity is limited to only 0.5 GWh. The total construction cost amounts to 2.05 billion CNY/year, representing a 40.06% reduction compared to Case I.

Table 7: Case II planning results

	Capacity	Cost/billion CNY
New thermal power units	2.4 GW	1.55
ESS	0.5 GW/1 GWh	0.23
E_{Pg}	76,492.51 GWh	17.59
E_{Wc}	10,308.67 GWh	8.56
E_{Lc}	0.30 GWh	0.003
Total cost		27.933

Although Case II ensures full power supply adequacy and completely resolves power shortage issues, the high thermal power commitment in certain low net load scenarios results in insufficient downward regulation capability. The limited energy storage capacity, coupled with a lack of discharge headroom, prevents the energy storage system from functioning effectively, leading to inadequate downward flexibility in the system. Compared with Case I, this case exhibits a 48.04% increase in curtailed energy, causing a corresponding rise in power curtailment costs of 2.93 billion CNY/year. Due to the inability to fully integrate renewable generation, thermal power output must increase by 3562.10 GWh to meet electricity demand, resulting in an additional 0.82 billion CNY/year in coal consumption costs. The annual operating cost reaches 26.73 billion CNY/year, an increase of 14.28%. Consequently, the total annualized cost rises by 1.97 billion CNY/year compared to Case I.

4.4 Case III Planning Results

In this case study, the scenario with the highest probability within each typical day is selected, and its maximum net load value is used to determine the daily unit commitment for thermal power units. The resulting thermal power committed capacities are presented in the Table 8, while the corresponding scenario probabilities can be found in Appendix A Table A1.

Table 8: Daily unit commitment for Case III

Day	1	2	3	4	5
Daily unit commitment (GW)	12	14.7	17.4	18.9	12.9

As shown in Table 8, in Case III where the unit commitment is determined based on the most probable scenario, the resulting daily commitment levels across all typical days are less than or equal to those in Case II, and exceed those in Case I in all cases except for Typical Day 2. This approach essentially yields a commitment strategy tailored to a single specific scenario, without accounting for renewable energy fluctuations in other scenarios.

The planning results for Case III are summarized in Table 9. This case yields the lowest construction cost for new equipment at only 1.78 billion CNY/year. However, compared to Case I, its operating cost is significantly higher at 26.15 billion CNY/year, representing an increase of 11.8%. Since the unit commitment strategy is derived from a single scenario without considering other potential renewable energy scenarios, the system requires greater energy storage capacity and power rating to maintain power supply reliability compared to Case II, despite both cases avoiding power shortages.

Table 9: Case III planning results

	Capacity	Cost/billion CNY
New thermal power units	24 GW	12.00
ESS	0.5 GW/1.5 GWh	2.5
E_{Pg}	763.45 billion kWh	175.59
E_{Wc}	101.61 billion kWh	84.33
E_{Lc}	0	0
Total cost		274.42

From an economic perspective, the total cost of this case falls between those of Case I and Case II. Regarding operational costs, however, while Cases II and III show minimal difference, Case I demonstrates a clear advantage.

4.5 Production Simulation Analysis for Typical Days

This section presents a comparative analysis of all scenarios in Typical Day 2 and Typical Day 3, examining the operational performance of equipment under the three planning cases. First, Fig. 9 illustrates the net load profiles for all scenarios in Typical Day 2.

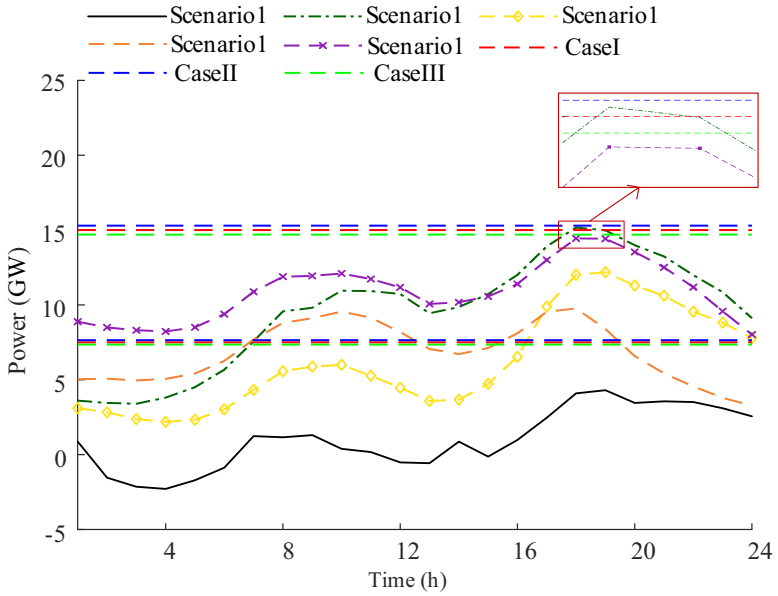

Figure 9: Net load profiles for all scenarios in typical day 2

For Typical Day 2, the total load energy consumption amounts to 335 GWh with an average load of 13.95 GW. Across the renewable energy scenarios, the penetration rate ranges from 20.06% to 83.72%. Scenario 1 exhibits the highest penetration rate, while Scenario 5 shows the lowest; notably, Scenario 5 also has the highest probability of occurrence.

As shown in Table 10, during Typical Day 2, all three cases successfully avoid power shortages. Case I achieves the lowest expected thermal power generation and the lowest expected wind curtailment among

the three strategies. In Scenario 5, which has the highest probability of occurrence, all three cases—with support from their respective energy storage systems—operate without any power curtailment or shortage. In Scenario 1, characterized by the highest renewable energy penetration, Case III, which employs the lowest committed capacity, results in the minimum curtailment volume across all cases. However, given the very low probability of Scenario 1 and its significant deviation in RE penetration from other scenarios, its overall impact on the typical day remains limited. In the remaining scenarios, Case I consistently demonstrates the lowest levels of both thermal power generation and renewable energy curtailment. A detailed analysis based on the production simulation results for Scenario 4 is provided below.

Table 10: Comparison of operational results across cases for typical day 2

Scenario		1	2	3	4	5	Expectation
Pg/GWh	Case I	180.00	242.47	194.76	180.00	260.49	219.31
	Case II	183.60	250.60	204.31	194.53	260.49	226.33
	Case III	176.40	248.45	199.24	189.43	260.49	223.33
Wc/GWh	Case I	155.69	13.11	46.65	15.31	0.00	21.95
	Case II	159.29	21.23	56.20	29.84	0.00	28.97
	Case III	152.09	19.08	51.13	24.74	0.00	25.97
Lc/GWh	Case I	0.00	0.00	0.00	0.00	0.00	0.00
	Case II	0.00	0.00	0.00	0.00	0.00	0.00
	Case III	0.00	0.00	0.00	0.00	0.00	0.00

As shown in Fig. 10, subfigures (a–c) illustrate the power balance conditions for the three cases, respectively. In Scenario 4, which has a renewable energy penetration rate of 50.83%, the net load remains at a relatively low level throughout. In Case I, the sufficient energy storage capacity enables the absorption of surplus renewable energy during low net load periods (e.g., hours 1–6), thereby reducing power curtailment. During high net load periods (e.g., hours 7–12), the system maintains low thermal power output while preserving discharge headroom for the energy storage system. This approach reduces generation from thermal power units and enhances renewable energy integration. In Scenario 4, the total curtailed energy in Case I amounts to 15.31 GWh, representing reductions of 48.68% compared to Case II and 38.10% compared to Case III.

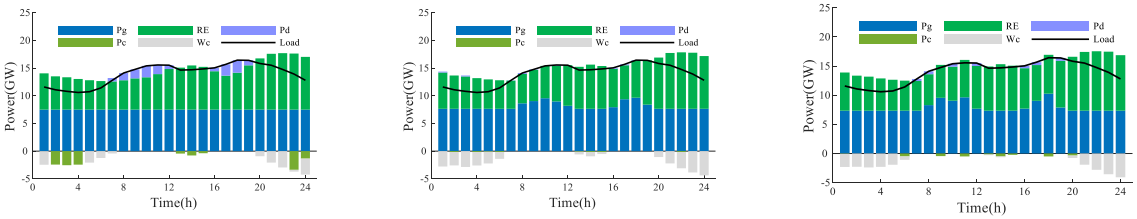

Figure 10: Scenario 4 production simulation results: (**a**) Case I; (**b**) Case II; (**c**) Case III

In summary, for Typical Day 2, Case I demonstrates significant advantages in high-probability scenarios. It successfully avoids power shortages while simultaneously reducing thermal power generation and enhancing renewable energy utilization. Specifically, compared to Case II, Case I reduces energy curtailment

by 24.2% and decreases thermal power generation by 3.10% throughout the typical day. When compared to Case III, it achieves reductions of 15.46% in curtailment and 1.80% in thermal generation.

The net load profiles for all scenarios in Typical Day 3 are presented in Fig. 11, while the corresponding production simulation results are summarized in Table 11.

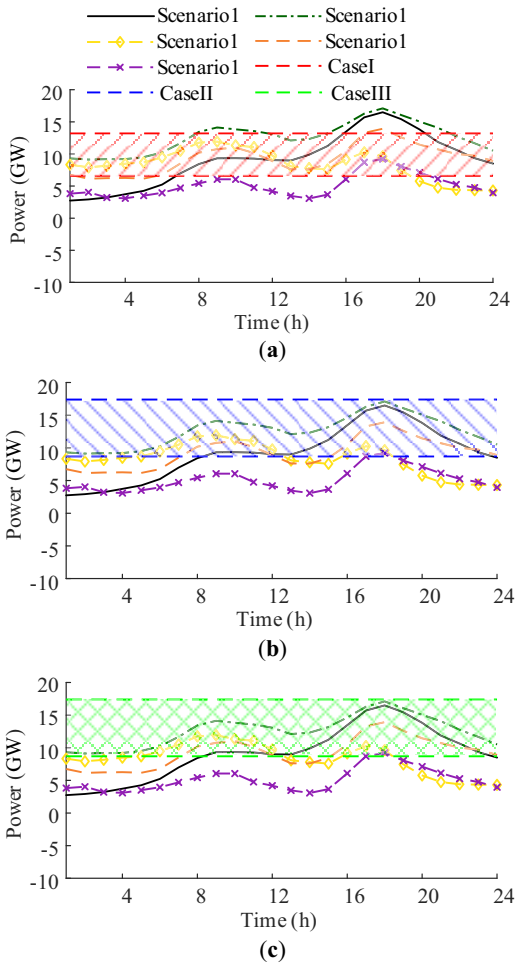

Figure 11: Net load profiles by scenario in typical day 3: **(a)** Case I; (**b**) Case II; (**c**) Case III

Table 11: Comparison of operational performance across cases for typical day 2

Scenario		1	2	3	4	5	Expectation
Pg/GWh	Case I	229.97	300.08	205.59	222.58	158.40	245.55
	Case II	251.74	302.11	225.73	238.36	209.14	262.26
	Case III	251.43	302.11	224.83	237.63	208.81	261.96
Wc/GWh	Case I	10.06	0.00	4.68	0.00	36.13	7.91
	Case II	31.82	0.00	24.81	15.78	86.87	23.72
	Case III	31.52	0.00	23.91	15.05	86.54	23.42
Lc/GWh	Case I	0.00	2.03	0.00	0.00	0.00	0.90
	Case II	0.00	0.00	0.00	0.00	0.00	0.00

(Continued)

Table 11 (continued)

Scenario		1	2	3	4	5	Expectation
	Case III	0.00	0.00	0.00	0.00	0.00	0.00

For Typical Day 3, the total load energy consumption reaches 371 GWh with an average load of 15.46 GW. The renewable energy penetration rate across scenarios ranges from 18.56% to 67.04%. Scenario 5 exhibits the highest penetration rate at 15.56% probability, while Scenario 2 shows the lowest penetration rate but the highest probability of occurrence at 44.44%.

As summarized in Table 11, during Typical Day 3, Case I—which also adopts a relatively conservative unit commitment—achieves reductions in both thermal power generation and energy curtailment across most scenarios. However, it experiences a minor power shortage in Scenario 2. Given the limited magnitude of this shortage, the resulting economic impact remains marginal. The production simulation results for Scenario 2 and Scenario 4 are analyzed in detail below.

Fig. 12 illustrates the power balance results for Scenario 2. In Case I, the minimal unit commitment results in the net load exceeding the maximum output capacity of the thermal power units during peak hours (16–21 h). However, with support from the energy storage system, only a minor power shortage occurs. The total energy shortage in this scenario amounts to 0.203 GWh, whereas no power shortages are observed in other scenarios where the net load also surpasses the thermal generation limit.

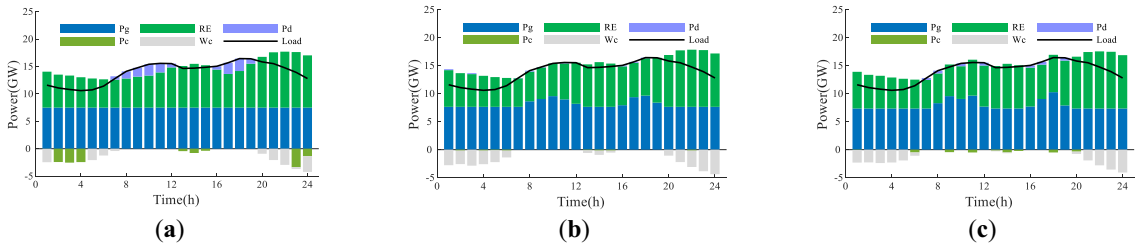

Figure 12: Production simulation results for scenario 2: (**a**) Case I; (**b**) Case II; (**c**) Case III

Fig. 13 illustrates the power balance results for Scenario 4. In this scenario, Case I completely eliminates both power curtailment and power shortage, demonstrating clear advantages over the other two cases.

For Typical Day 3, compared to Case II, Case I reduces energy curtailment by 66.65% and decreases thermal power generation by 6.37%. When compared to Case III, it achieves reductions of 66.22% in curtailment and 6.26% in thermal generation. Although Case I experiences a minor power shortage in Scenario 2, the overall expected energy shortage across Typical Day 3 amounts to only 0.9 GWh.

The expected operating costs for all cases across the typical days are summarized in Figs. 6 and 14, while detailed values for thermal power generation, curtailed energy, and power shortage are provided in Appendix A Table A2.

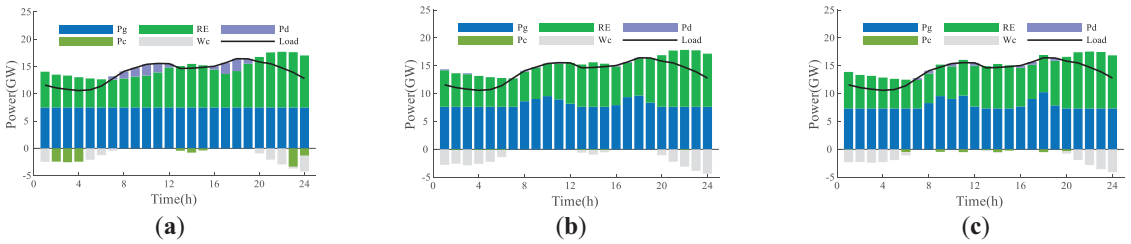

Figure 13: Production simulation results for scenario 4: (**a**) Case I; (**b**) Case II; (**c**) Case III

As shown in Fig. 14, employing the entropy weight method to determine the daily unit commitment for thermal power units enables coordinated planning with energy storage systems. This approach effectively balances the dual requirements of ensuring power supply reliability and promoting renewable energy utilization under multiple renewable energy uncertainty scenarios, while simultaneously reducing overall system operating costs.

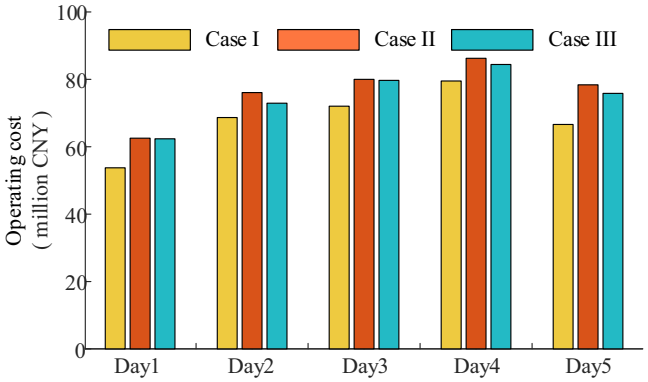

Figure 14: Summary of operating costs of each typical day

5 Conclusion

This paper proposes a coordinated thermal power-energy storage planning methodology to address the challenges posed by multiple renewable energy uncertainty scenarios in future power systems. The main conclusions are as follows:

(1) The entropy weight method is employed to determine the daily unit commitment of conventional thermal power units, forming the basis for coordinated thermal power-energy storage planning. The resulting planning scheme effectively balances power supply security and renewable energy utilization across multiple scenarios.

(2) Future power systems with high renewable energy penetration will face “one-to-many” relationships between load profiles and renewable energy scenarios. A unit commitment strategy derived from a single scenario may lead to unnecessary curtailment or shortage losses in other scenarios. Therefore, appropriate unit commitment strategies combined with energy storage deployment enable systems to flexibly accommodate renewable energy uncertainties.

(3) Comparative analysis with the maximum net load method and the most probable scenario method demonstrates the effectiveness of the proposed approach. The methodology achieves cost savings and reduced curtailment across all typical days, with only minor power shortages occurring in extremely low renewable energy scenarios during Typical Day 3, accounting for merely 0.32% of the daily total

load—manageable through demand-side response measures. Compared to Case II, the total planning period cost is reduced by 6.84%, and by 4.02% compared to Case III.

Acknowledgement: This research was supported by Science and Technology Project of the headquarters of the State Grid Corporation of China.

Funding Statement: This research was supported by Science and Technology Project of the headquarters of the State Grid Corporation of China, grant number No. 4000-202399368A-2-2-ZB.

Author Contributions: Conceptualization: Xiuyu Yang, Cheng Yang; data curation: Cheng Yang; formal analysis: Cheng Yang, Gangui Yan; funding acquisition: Hongda Dong, Chenggang Li; investigation: Hongda Dong, Chenggang Li; methodology: Xiuyu Yang, Cheng Yang, Gangui Yan; project administration: Hongda Dong; resources: Chenggang Li; software: Cheng Yang, Chenggang Li; supervision: Xiuyu Yang, Hongda Dong; validation: Hongda Dong, Chenggang Li; visualization: Cheng Yang; writing—original draft: Cheng Yang; writing—review & editing: Xiuyu Yang, Cheng Yang, Gangui Yan. All authors reviewed the results and approved the final version of the manuscript.

Availability of Data and Materials: Due to the nature of this research, participants of this study did not agree for their data to be shared publicly, so supporting data is not available.

Ethics Approval: Not applicable. For studies not involving humans or animals.

Conflicts of Interest: The authors declare no conflicts of interest to report regarding the present study.

Abbreviations

RE Renewable Energy
ESS Energy Storge System
SoC State of Charge

Appendix A

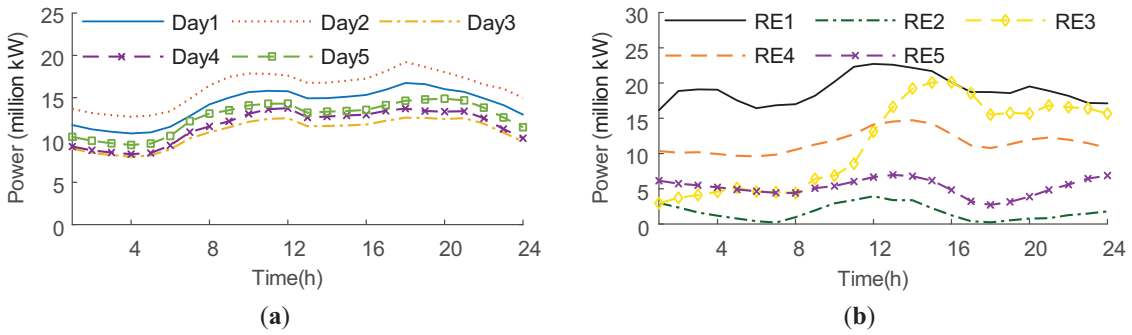

(a) (b)

Figure A1: (Continued)

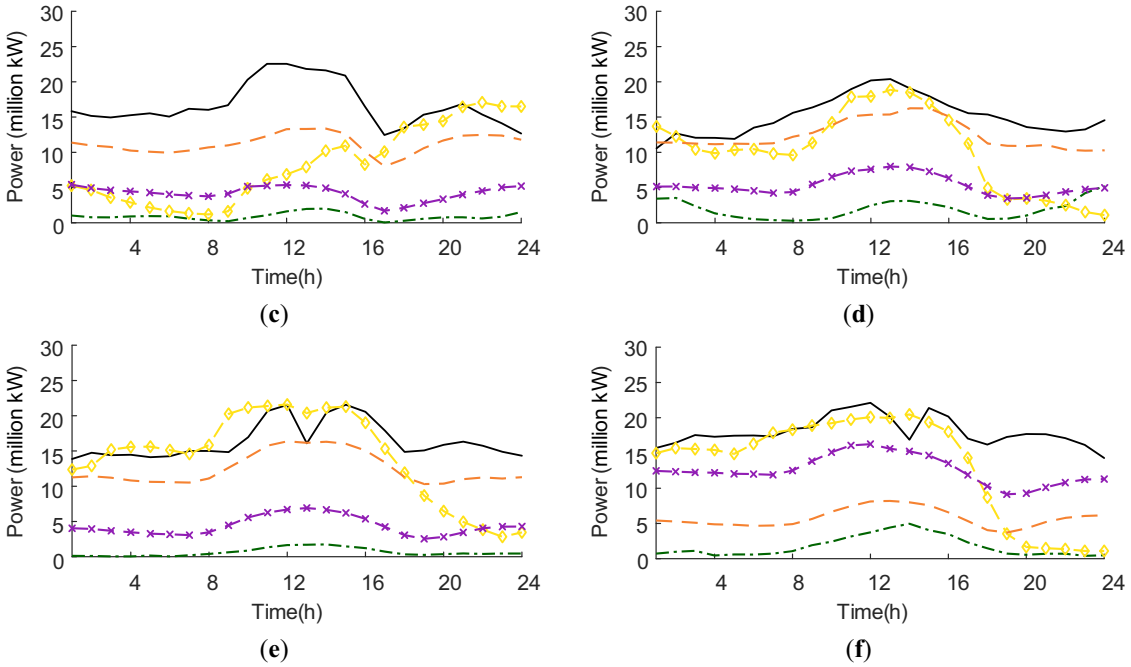

Figure A1: Load and renewable energy profiles for typical days (**a**) Load; (**b**) RE in Day1; (**c**) RE in Day2; (**d**) RE in Day3; (**e**) RE in Day4; (**f**) RE in Day5

Table A1: Scenario probabilities within each typical day

	Scenario 1	Scenario 2	Scenario 3	Scenario 4	Scenario 5
Day 1	13.82%	19.51%	13.01%	9.76%	43.90%
Day 2	4.05%	10.81%	21.62%	27.03%	36.49%
Day 3	15.56%	44.44%	15.56%	8.89%	15.56%
Day 4	20.00%	25.00%	15.00%	10.00%	30.00%
Day 5	40.78%	20.39%	10.68%	19.42%	8.74%

Table A2: Production simulation results for typical days

Day		C_{Pg}/GWh	C_{Wc}/GWh	C_{Lc}/GWh
1	I	177.14	15.68	0.00
	II	185.44	23.98	0.00
	III	185.26	23.80	0.00
2	I	219.31	21.95	0.00
	II	226.33	28.97	0.00
	III	223.33	25.97	0.00
3	I	245.55	7.91	0.90
	II	262.26	23.72	0.00
	III	261.96	23.42	0.00

(Continued)

Table A2 (continued)

Day		C_{Pg}/GWh	C_{Wc}/GWh	C_{Lc}/GWh
4	I	309.88	9.94	0.00
	II	316.24	16.30	0.00
	III	314.35	14.43	0.02
5	I	176.79	31.28	0.00
	II	187.88	42.38	0.00
	III	185.48	39.97	0.00

Appendix B

Appendix B.1 Thermal Power Unit Constraints

$$U^{\min} \le P_{g,t} \le U^{\max} \tag{A1}$$

$$RD \le P_{g,t} - P_{g,t-1} \le RU \tag{A2}$$

where, $U^{\min}$ and $U^{\max}$ are the upper and lower limits of the output of the thermal power unit under the selected comprehensive startup plan; $P_{g,t}$ represents the output of thermal power unit at time t; RU, RD are the power limits for upward and downward ramping of thermal power units.

Appendix B.2 Renewable Energy Unit Constraints

$$0 \le W_t \le {W_t}^{\max} \tag{A3}$$

$$0 \le W_{c,t} \le {W_t}^{\max} \tag{A4}$$

where, W_t is the actual output of renewable energy at time t, and ${W_t}^{\max}$ is the upper limit of renewable energy output; $W_{c,t}$ is the renewable energy curtailment at time t.

Appendix B.3 Energy Storage Constraints

$$0 \le P_{\mathrm{ch},t} \le P_{\mathrm{ess}} n_{\mathrm{ch},t} \tag{A5}$$

$$0 \le P_{\mathrm{dis},t} \le P_{\mathrm{ess}} n_{\mathrm{dis},t} \tag{A6}$$

$$n_{\mathrm{ch},t} + n_{\mathrm{dis},t} = 1 \tag{A7}$$

where, $P_{\mathrm{ch},t}$, $P_{\mathrm{dis},t}$ are the charging and discharging power of the energy storage device at time t, respectively; $n_{\mathrm{ch},t}$, $n_{\mathrm{dis},t}$ are the charge and discharge state of the energy storage device at time t.

$$\mathrm{SoC}_t = \mathrm{SoC}_{t-1} + \left(P_{\mathrm{ch},t}\eta_{\mathrm{ch}} - P_{\mathrm{dis},t}/\eta_{\mathrm{dis}}\right)\Delta t \tag{A8}$$

$$\mathrm{SoC}^{\min} \le \mathrm{SoC}_t \le \mathrm{SoC}^{\max} \tag{A9}$$

$$\mathrm{SoC}_{24} = \mathrm{SoC}_{\mathrm{ini}} \tag{A10}$$

where, SoC_t is the state of charge of the energy storage device at time t, η_{ch}, η_{dis} are the charging and discharging efficiency of the energy storage device, respectively, and Δt is the unit time, which is 1 h; $\mathrm{SoC}^{\max}$, $\mathrm{SoC}^{\min}$ limit the maximum and minimum interval of the state of charge of the energy storage; the $\mathrm{SoC}_{\mathrm{ini}}$ is the initial state of charge of the energy storage device.

Appendix B.4 Power Conservation Constraints

$$P_{g,t} + W_t + P_{\mathrm{dis},t} + L_{c,t} = L_t + P_{\mathrm{ch},t} \tag{A11}$$

$$W_{c,t} + W_t = W^{\max} \tag{A12}$$

$$L_{c,t} \le L_t \tag{A13}$$

where, $L_{c,t}$ is the load shedding power at time t.

Table A3: Basic parameters of calculation example

Parameter name	Value
Thermal power unit capacity/GW	0.30
Thermal power unit construction cost/(million CNY/GW)	500.00
Climbing rate of thermal power unit/p.u.	0.17
Coal-fired cost of thermal power unit/(CNY/kWh)	0.28
The penalty cost of power curtailment/(CNY/kWh)	0.83
The penalty cost of power shortage/(CNY/kWh)	10.00
Energy storage unit capacity cost/(million CNY/GWh)	150.00
Converter unit power cost/(million CNY/GW)	50.00
Energy storage charging efficiency/%	95
Energy storage discharging efficiency/%	95
Upper SoC Limit for Energy Storage	0.95
Lower SoC Limit for Energy Storage	0.05
Planning cycle/year	20.00
Discount rate/%	5

References

1. Kang CQ, Du ES, Guo HY, Li YW, Fang YC, Zhang N, et al. Primary exploration of six essential factors in new power system. Power Syst Technol. 2023;47(5):1741–50. (In Chinese). doi:10.13335/j.1000-3673.pst.2023.0535.
2. Ding J, Xie K, Hu B, Shao C, Niu T, Li C, et al. Mixed aleatory-epistemic uncertainty modeling of wind power forecast errors in operation reliability evaluation of power systems. J Mod Power Syst Clean Energy. 2022;10(5):1174–83. doi:10.35833/mpce.2020.000861.
3. Kaushik E, Prakash V, Mahela OP, Khan B, El-Shahat A, Abdelaziz AY. Comprehensive overview of power system flexibility during the scenario of high penetration of renewable energy in utility grid. Energies. 2022;15(2):516. doi:10.3390/en15020516.
4. Hu YX, Wang MQ, Yang M, Wang MX, Zhao LM, Ding TC, et al. Economic dispatch of active distribution network considering admissible region of net load based on new injection shift factors. Int J Electr Power Energy Syst. 2023;145(2):108641. doi:10.1016/j.ijepes.2022.108641.
5. Li Z, Wang C, Li B, Wang J, Zhao P, Zhu W, et al. Probability-interval-based optimal planning of integrated energy system with uncertain wind power. IEEE Trans Ind Appl. 2020;56(1):4–13. doi:10.1109/tia.2019.2942260.
6. Guo Q, Nojavan S, Lei S, Liang X. Economic-environmental analysis of renewable-based microgrid under a CVaR-based two-stage stochastic model with efficient integration of plug-in electric vehicle and demand response. Sustain Cities Soc. 2021;75:103276. doi:10.1016/j.scs.2021.103276.
7. Huang S, Sun Y, Wu Q. Stochastic economic dispatch with wind using versatile probability distribution and L-BFGS-B based dual decomposition. IEEE Trans Power Syst. 2018;33(6):6254–63. doi:10.1109/TPWRS.2018.2834433.

8. Guo X, Chen X, Chen X, Sherman P, Wen J, McElroy M. Grid integration feasibility and investment planning of offshore wind power under carbon-neutral transition in China. Nat Commun. 2023;14(1):2447. doi:10.1038/s41467-023-37536-3.
9. Liu D, Zhang S, Cheng H, Liu L, Wang Z, Sang D, et al. Accommodating uncertain wind power investment and coal-fired unit retirement by robust energy storage system planning. CSEE J Power Energy Syst. 2020;8(5):1398–407. doi:10.17775/cseejpes.2019.01890.
10. Wang Z, Xuan A, Shen X, Du Y, Sun H. A robust planning model for offshore microgrid considering tidal power and desalination. Appl Energy. 2023;350(4):121713. doi:10.1016/j.apenergy.2023.121713.
11. Yan C, Geng X, Bie Z, Xie L. Two-stage robust energy storage planning with probabilistic guarantees: a data-driven approach. Appl Energy. 2022;313(2):118623. doi:10.1016/j.apenergy.2022.118623.
12. He G, Ciez R, Moutis P, Kar S, Whitacre JF. The economic end of life of electrochemical energy storage. Appl Energy. 2020;273:115151. doi:10.1016/j.apenergy.2020.115151.
13. Elalfy DA, Gouda E, Kotb MF, Bureš V, Sedhom BE. Comprehensive review of energy storage systems technologies, objectives, challenges, and future trends. Energy Strategy Rev. 2024;54(45):101482. doi:10.1016/j.esr.2024.101482.
14. Orfanos GA, Georgilakis PS, Hatziargyriou ND. Transmission expansion planning of systems with increasing wind power integration. IEEE Trans Power Syst. 2013;28(2):1355–62. doi:10.1109/TPWRS.2012.2214242.
15. Villumsen JC, Brønmo G, Philpott AB. Line capacity expansion and transmission switching in power systems with large-scale wind power. IEEE Trans Power Syst. 2013;28(2):731–9. doi:10.1109/TPWRS.2012.2224143.
16. Valdez Castro JM, Aguila Téllez A. Strategic planning for power system decarbonization using mixed-integer linear programming and the William Newman model. Energies. 2025;18(18):5018. doi:10.3390/en18185018.
17. Haugen M, Farahmand H, Jaehnert S, Fleten SE. Representation of uncertainty in market models for operational planning and forecasting in renewable power systems: a review. Energy Syst. 2023;1–36. doi:10.1007/s12667-023-00600-4.
18. Aupke P, Kassler A, Theocharis A, Nilsson M, Uelschen M. Quantifying uncertainty for predicting renewable energy time series data using machine learning. Eng Proc. 2021;5(1):50. doi:10.3390/engproc2021005050.
19. Fu Y, Bai H, Cai Y, Yang W, Li Y. Optimal configuration method of demand-side flexible resources for enhancing renewable energy integration. Sci Rep. 2024;14(1):7658. doi:10.1038/s41598-024-58266-6.
20. Wu J, Wang H, Wang W, Zhang Q. Performance evaluation for sustainability of wind energy project using improved multi-criteria decision-making method. J Mod Power Syst Clean Energy. 2019;7(5):1165–76. doi:10.1007/s40565-019-0517-6.
21. Wang Y, Zhou X, Liu H, Chen X, Yan Z, Li D, et al. Evaluation of the maturity of urban energy Internet development based on AHP-entropy weight method and improved TOPSIS. Energies. 2023;16(13):5151. doi:10.3390/en16135151.